Transcriptome analysis of root-knot nematode (Meloidogyne incognita)-infected tomato (Solanum lycopersicum) roots reveals complex gene expression profiles and metabolic networks of both host and nematode during susceptible and resistance responses

Shukla, Neha; Yadav, Rachita; Kaur, Pritam; Rasmussen, Simon; Goel, Shailendra; Agarwal, Manu; Jagannath, Arun; Gupta, Ramneek; Kumar, Amar

Published in:
Molecular Plant Pathology

Link to article, DOI:
10.1111/mpp.12547

Publication date:
2018

Document Version
Peer reviewed version

Transcriptome analysis of root-knot nematode (*Meloidogyne incognita*)-infected tomato (*Solanum lycopersicum*) roots reveals complex gene expression profiles and metabolic networks of both host and nematode during susceptible and resistance responses

Neha Shukla[1], Rachita Yadav[2], Pritam Kaur[1], Simon Rasmussen[2], Shailendra Goel[1], Manu Agarwal[1], Arun Jagannath[1], Ramneek Gupta[2] and Amar Kumar[1*]

[1]Department of Botany, University of Delhi, Delhi 110007, India; [2]Department of Bio and Health Informatics, Technical University of Denmark, Kemitorvet 208, 2800, Lyngby, Denmark

Author for correspondence:

Amar Kumar

Tel: +919871515733

Email: akumar23j@gmail.com

Running Title: **Transcriptome RKN-infected tomato roots**

Key words: Transcriptome, Effectors, Tomato roots, *Meloidogyne incognita* (RKN), Susceptible, Resistance, Metabolic networks

Total Word count (including Summary, Introduction, Results, Discussion, Experimental Procedures, Acknowledgements, Table and Figure Legends):	7802	No. of Figures:8	
Summary:		No. of Tables:	1
Introduction:	792	No. of Supporting Information files:	23 (Fig. S1-S17; Table S1-S6)
Results:	2274		
Discussion:	2207		
Experimental procedures:	9		
Acknowledgements:	72		

This article has been accepted for publication and undergone full peer review but has not been through the copyediting, typesetting, pagination and proofreading process which may lead to differences between this version and the Version of Record. Please cite this article as an 'Accepted Article', doi: 10.1111/mpp.12547

Transcriptome analysis of root-knot nematode (*Meloidogyne incognita*)-infected tomato (*Solanum lycopersicum*) roots reveals complex gene expression profiles and metabolic networks of both host and nematode during susceptible and resistance responses

Summary

Root knot nematodes (RKNs, *Meloidogyne incognita*) are economically important endoparasites having a wide-host range. We have taken a comprehensive transcriptomic approach to investigate the expression of both tomato and RKN genes in tomato roots at five infection time intervals from susceptible plants and two infection time intervals from resistant plants, grown under soil conditions. Differentially expressed genes during susceptible (1827-tomato, 462-RKN) and resistance (25-tomato, 160-RKN) interactions were identified. In susceptible responses, tomato genes involved in cell wall structure, development, primary and secondary metabolites and defense signalling pathways along with RKN genes involved in host parasitism, development and defense are discussed. In resistance responses, tomato genes involved in secondary metabolite and hormone-mediated defense responses along with RKN genes involved in starvation stress-induced apoptosis are discussed. Also, forty novel differentially expressed RKN genes encoding secretory proteins were identified. Our findings, for the first time, provide novel insights into temporal regulation of genes involved in various biological processes from tomato and RKN simultaneously during susceptible and resistance responses, and reveals involvement of a complex network of biosynthetic pathways during disease development.

Introduction

Root-knot nematodes (RKN; *Meloidogyne spp.*) are devastating polyphagous endoparasites that parasitize many cultivated plants worldwide and pose a serious threat to global food security. The estimated crop losses due to RKN infections are over 100 billion dollars annually (Trudgill & Blok, 2001). RKNs are highly sophisticated parasites that hijack host machinery, by secreting

effector molecules, to initiate and maintain feeding cells inside the host roots in order to complete their life cycle within 4-6 weeks (Abad & Williamson, 2010). The effector molecules consist of enzymes, peptides, small metabolites or other biomolecules, and have many roles in plant parasitism (Mitchum *et al.*, 2013, Shukla *et al.*, 2016). Majority of effector molecules are produced in the oesophageal glands (two sub-ventral and one dorsal) while others are synthesized in hypodermis and amphids. Effectors have been identified using various approaches such as EST or genomic datasets and direct sequencing of gland cell mRNA (Huang *et al.*, 2003; Bellafiore *et al.* 2008; Rutter *et al.*, 2014a). A number of RKN effectors, including cellulases, xylanases, annexins, expansins, calreticulin, fatty-acid retinol binding (FAR) protein and chorismate mutase have previously been characterized (Huang *et al.*, 2005; Jaubert *et al.*, 2005; Haegeman *et al.*, 2013; Jaouannet *et al.*, 2013; Truong *et al.*, 2015).

The zig-zag model of plant immune system professes two branches of pathogen induced plant defense responses, pattern-triggered immunity (PTI) and effector-triggered immunity (ETI) (Jones & Dangl, 2006). Recently, members of a conserved family of nematode pheromones (ascarosides) have been identified as nematode pathogen-associated molecular patterns (PAMPs) (Manosalva *et al.*, 2015). The resistance gene (R gene) from tomato, *Mi-1.2*, which belongs to nucleotide binding site–leucine rich repeat (NBS-LRR) class, activates ETI and confers resistance against three species of *Meloidogyne* (Milligan *et al.*, 1998). Direct or indirect interaction of *Mi*-gene with an as yet unknown avirulence (Avr) protein, elicits a cascade of signal transduction pathways that activate defense responses (Hwang & Williamson, 2003; Williamson & Kumar, 2006). Previous studies have reported that *Mi*-mediated resistance is characterized by localized cell death when second stage juvenile (J2) attempts to establish feeding site inside the host roots (Williamson & Hussey, 1996). As a result, development of feeding site is impaired and unable to supply nutrition to nematodes. Prior studies have reported the involvement of mitogen-activated protein kinase (MAPK) signalling cascades, resulting in production of reactive oxygen species (ROS) and participation of *Rme*1 gene for activation of

defense responses including salicylic acid (SA) and ethylene (ET) signalling pathways (de Ilarduya *et al.*, 2001; Branch *et al.*, 2004; Li *et al.*, 2006; Bhattarai *et al.*, 2008; Mantelin *et al.*, 2013, Molinari *et al.*, 2013).

Transcriptomic changes occurring either in susceptible or resistant plants during host-RKN interaction have been studied using various approaches such as RNA blotting, differential cDNA library screening, EST sequencing, microarrays and more recently, next generation sequencing (NGS) (Abad & Williamson, 2010). Microarray-based transcriptome studies have been conducted in *Arabidopsis* (Hammes *et al.*, 2005; Jammes *et al.*, 2005; Fuller *et al.*, 2007; Barcala *et al.*, 2010), tomato (Bar-Or *et al.*, 2005; Schaff *et al.*, 2007; Portillo *et al.*, 2013), a resistant soybean line (Ibrahim *et al.*, 2011) and RKN tolerant egg-plant *Solanum torvum* (Bagnaresi *et al.,* 2013). To date, only a few studies have utilized NGS to investigate differential host gene expression patterns during RKN-host interaction including rice galls and giant cells (GCs) (Kyndt *et al.*, 2012; Ji *et al.*, 2013), resistant soybean roots (Beneventi *et al.*, 2013), resistant and susceptible alfalfa cultivars (Postnikova *et al.*, 2015) and common bean roots (Santini *et al.,* 2016). However, previous studies were either on the host or dissected nematodes with limited number of disease developmental stages. Only one study to date has reported both host and nematode genes from resistant and susceptible cultivars with RKN-infected alfalfa roots grown in *in vitro* conditions and with a limited number of infective stages (Postnikova *et al.*, 2015).

The availability of relatively well annotated genome reference sequences of both tomato and RKN have made the tomato-RKN system an excellent crop model for studying host-pathogen interactions. In this study, we investigated the expression profiles of both tomato and RKN genes from *in vivo* infected tomato roots under soil-grown conditions at five infection time intervals in a susceptible line and two infection time intervals in a resistant line. The study revealed complex changes in genes involved in cell wall architecture, development, hormonal signalling cascades and defense responses elicited by RKN in susceptible and resistant tomato roots. Also, the repertoire of RKN genes that are most likely involved in parasitism, nematode

growth, development and defense is presented. To the best of our knowledge, this is the first comprehensive study that highlights simultaneously the expression profiles of tomato and RKN during susceptible and resistant responses in *in vivo* RKN-infected tomato roots under soil-grown conditions.

Results

Sequencing data and transcriptome mapping

Experiments were conducted to study life cycle of RKN inside tomato roots and for a selection of disease developmental stages (Fig. 1). Transcriptome sequencing generated 1,154,560,291 paired-end reads for replicate 1 and 537,461,341 single-end reads for replicate 2 of 100 bp in length. Quality filtering of raw reads was done for mean phred quality score of 20 and any contaminating adapter sequences were removed (Table S1). For both the replicates, 95%-99% good quality 35-88 bp reads were retained, which were used for mapping onto reference genome using TopHat2. In total, 72%-92% of good quality reads were mapped onto *S. lycopersicum* genome (SL2.50 assembly) across all samples (Table 1). For infected samples, 0.1%-6.3% of reads were mapped to *M. incognita* genome (Table 1). All the sequencing data, raw data as well as the processed data, have been submitted to Gene Expression Omnibus (GEO) repository on NCBI with accession no. GSE88763 and SRA accession no. SRP091567.

Identification of tomato genes from susceptible tomato (PR) and resistant tomato (M36) plants

Differential gene expression analysis and annotations

Five different stages of infection and their corresponding uninfected controls were selected to study susceptible response during RKN infection in tomato roots. A total of 24,411 tomato genes were identified across these five stages. Stage-wise comparison of infected roots with their corresponding uninfected controls identified a total of 1,827 significant DEGs (adjusted p-value

< 0.05 and $\log_2$ fold change ≥±2) (Fig. 2a; Table S2). No significant DEGs were identified at stage 1. Eighteen significant DEGs were identified at stage 2 with more genes showing up-regulation than down-regulation. At stage 3, 905 significant DEGs were obtained. At stage 4 and stage 5, 1,054 DEGs and 1,308 DEGs were identified respectively, with more genes showing down-regulation (56.8% and 55.9% respectively).

In resistant plants, only first two stages of infection (stages 1, 2) and corresponding uninfected controls were selected for the study. A total of 23,393 tomato genes were identified across two stages of infection. Stage-wise comparison of infected roots with their corresponding uninfected controls identified no significant DEGs at stage 1 and only 25 at stage 2; with 21 up-regulated and 4 down-regulated genes (Table S3). Additionally, we compared significant DEGs obtained from susceptible and resistance responses. Since no significant DEG was observed at stage 1, DEGs obtained at stage 2 (18 in susceptible response and 25 in resistance response), were compared. Only two up-regulated genes were common at stage 2 between susceptible and resistance responses, one encodes mitochondrial trans-2-enoyl-CoA reductase and the other encodes major latex-like protein, while rest of the genes were distinct (Fig. 2b). Additionally, quantitative PCR was performed to validate the expression profiles of tomato genes, including glucan endo-1,3-beta-glucosidase in susceptible response and receptor-like kinase in resistance response (Fig. 2c,d).

Furthermore, sample to sample correlation was observed based on global gene expression profiles of genes identified across all stages in susceptible response (Fig. S1). Gene ontology annotation and protein classes annotation of DEGs in both susceptible and resistance responses was performed (Fig. S2, S3, S4). Gene set enrichment analysis revealed significant results in molecular function category only at two stages (stages 4, 5) during susceptible response (Fig. S5).

Differential regulation of genes resulting in altered cell wall architecture

Our data reflects significant alteration in expression of 85 tomato genes involved in cell wall degradation (43 genes), cell wall modification (29 genes), cell wall proteins (5 genes) and cell wall synthesis (8 genes) during susceptible responses (Fig. 3a; Fig. S6). By contrast, in resistant responses no significant alteration was observed in expression of genes involved in modulation of cell wall architecture.

Differential regulation of plant developmental genes and primary metabolism

During susceptible responses, 57 genes involved in plant cell cycle (3 genes), cytoskeletal organization (3 genes), root cap proteins (7 genes) and transcription factors controlling developmental processes (18 genes) were differentially expressed (Fig. 3b; Fig. S7). Furthermore, differential expression of 102 genes, involved in photosynthesis (12 genes), major and minor carbohydrate metabolism (9 genes), fermentation (5 genes), TCA cycle (4 genes), mitochondrial electron transport (1 gene), nitrogen metabolism (2 genes), amino acid metabolism (17 genes), tetrapyrrole synthesis (4 genes) nucleotide metabolism (12 genes) and lipid metabolism (36 genes) (Fig. 3c; Fig. S8a-d) was observed. By contrast, in resistant responses, a gene encoding patatin protein was up-regulated at stage 2 and no alteration was observed in genes involved in primary metabolism.

Differential regulation of transporter genes

The expression of solute transporter genes were altered in susceptible responses, which included various carbohydrate and sugar transporters (19 genes), lipid transporters (7 genes), aquaporins (13 genes), peptide, nitrate and amino acid transporters (18 genes) (Fig. 3d; Fig. S9a-d). Also, genes encoding multidrug and toxic compound extrusion (MATE) efflux transporters (15 genes), ATP-binding cassette (ABC) transporters (8 genes) and various ion transporters (32 genes) were altered (Fig. 3d; Fig. 9e,f). By contrast, no significant alteration was observed in resistance response.

Suppression of plant defense responses by alteration of secondary and phytohormone metabolisms

The secondary metabolite pathway analysis revealed alteration in biosynthetic pathways of various secondary metabolites that include phenylpropanoid pathway, flavonoid pathway, polyamine pathway and isoprenoid pathway (Fig. 4; Fig. S10a,b).

In the phenylpropanoid biosynthetic pathway, phenylalanine ammonia lyase (PAL) and 4-hydroxycinnamoyl CoA ligase (4CL) were up-regulated during disease development. Other downstream genes, including cinnamoyl alcohol dehydrogenase (CAD) and flavonol synthase were down-regulated (Fig. 4). We also found alterations in genes involved in isoprenoids and polyamine metabolisms along with down-regulation of 4 genes involved in gibberellin biosynthesis (Fig. S10a,b). Additionally, alteration in expression of genes involved in auxin signalling (16 genes) and cytokinin synthesis (4 genes) was observed (Fig. S11a). Abscisic acid (ABA) synthesis and responsive genes were also altered, including up-regulation of lycopene beta cyclase, FIP1 and HVA22-like protein c at stages 3-5 (Fig. S10a, Fig. S11b).

Genes coding for enzymes involved in ET biosynthesis and signalling, including 1-aminocyclopropane-1-carboxylic acid (ACC) synthase (ACS; 2 genes), ACC oxidase (ACO; 16 genes) and ethylene responsive transcription factors (ERFs; 32 genes) were differentially expressed (Fig. S10b, Fig. S12). Additionally, we found differential expression of genes involved in jasmonic acid (JA) synthesis (8 genes) and salicylic acid (SA) responsive signalling (8 genes) during disease development (Fig. S13a,b). Genes related to oxidative stress including glutathione S-transferases, peroxidases and thioredoxins were largely down-regulated upon RKN infection during later stages (Fig. S13c).

In resistant responses, we found up-regulation of a receptor-like kinase and protein phosphatase 2C (regulator of ABA signalling). An ABA responsive HVA22-like protein c and a salicylic acid carboxyl methyltransferase were also up-regulated at stage 2. Additionally, two ERFs were up-

regulated at stage 2 indicating active hormone-mediated defense responses (Fig. 2b).

Expression profiles of tomato genes validated through qRT-PCR

In total, 20 genes were selected (up-regulation or down-regulation) that showed significant fold change (≤ 2 or ≥ 2) for further validation by qRT-PCR (Table S4). A gene encoding an open reading frame (Solyc01g080500.2) and tubulin alpha chain (Solyc08g006890.2) showing uniform expression in all stages were used as internal controls for tomato. The gene expression patterns obtained through qPCR were coincident with RNASeq expression profiles. Correlation coefficient (R^2) was 0.80 at p-value of 2.2e-16 (Fig. S14).

Identification of root-knot nematode (RKN) genes from infected root samples of susceptible and resistant tomato plants

Reads aligned onto RKN genome and differential expression analysis

Good quality reads from infected samples of susceptible plants were aligned onto RKN genome (Table 1). Non-tomato mapped reads led to identification of 10,131 protein-encoding RKN genes. Hierarchical clustering of global expression profiles clustered the genes into two groups (Fig. S15).

In susceptible response, we identified 462 significant DEGs (adjusted p-value < 0.05 and $\log_2$ fold change ≥ 2) as compared to stage 1 (Fig. 5a, S16a,b; Table S5). Since same population of RKN was used to study susceptible and resistance responses, RKN predicted genes of the same stage from both interactions were compared. In resistant response, no significant alteration was found at stage 1 and 160 significant DEGs were identified at stage 2 as compared to susceptible response (Table S6).

Effector identification

A search for candidate effectors amongst 10,131 RKN mapped translated proteins using SignalP

4.1 followed by TMHMM 2.0, identified 675 proteins that have signal peptide sequence but no trans-membrane domain. Further, through manual screening based on reported putative effectors, we identified 157 putative effectors and 312 novel secretory molecules. Additionally, blast results identified additional 81 known effectors, out of which 8 were found to have signal peptide sequence only (Fig. 5b). We also looked for differential expression of these 559 candidate effectors at different stages during disease development in susceptible response. A total of 109 genes were differentially expressed (Fig. 5c), out of which 60 were previously reported as effectors and 49 could be classified as potentially secreted molecules with unknown functions.

Differential regulation of RKN genes encoding cell wall degrading enzymes and peptidases

We found significant expression of 10 members of glycosyl hydrolase (GH) and 6 members of pectate lyase (PL) families at stages 1, 2 during susceptible responses. Furthermore, expression of UDP-glucosyltransferase gene was significant at stages 1,2 and down-regulated at stages 3-5, whereas expression of gene encoding carboxylesterase was up-regulated at stages 3-5. The expression of a member of carbohydrate-binding module family 20 was specifically down-regulated at stages 3 and 5 (Fig. 6a). We also found stage-specific differential expression of 30 genes encoding different peptidases including aspartic, cysteine, metallo and serine peptidases (Fig. 6a). The expression of 6 genes encoding aspartic and serine peptidases were significant during stages 1-2, but later they were down-regulated. While expression of 8 genes coding for various peptidases were up-regulated at later stages. Also, expression of 5 genes encoding metallo and serine peptidases was significant at stages 2-4, but down-regulated at stage 5.

Interestingly, in resistance response, we observed up-regulation of 7 genes encoding members of GH family, 5 genes encoding members of PL family along with 7 genes encoding aspartic and cysteine peptidases at stage 2 as compared to susceptible responses (Table S6). The expression of 2 genes (out of 5) encoding aspartic peptidase and 1 gene (out of 2) encoding cysteine

peptidase was unique to resistance response.

Differential regulation of RKN genes involved in nematode development and metabolism

Genes encoding for 2 cuticle collagen and 5 tubulin proteins were up-regulated at stage 3 while none were up-regulated at stage 2. Expression of 16 cuticle collagens was induced at stage 4 indicating the dynamic transition and development of RKN into J4 and adult worms. Two genes coding for intermediate filament protein 1 (IFA-1) were up-regulated during all stages of RKN development, whereas 2 genes coding for calponin protein were down-regulated. In total, 17 genes encoding ribosomal proteins (RP) were found to be significantly altered during disease development. RPL29e was found to be down-regulated at stage 4, whereas other 16 genes were up-regulated at stage 3 only (Fig. 6b). By contrast, in resistant responses, expression of cuticle collagens was not significantly altered. Additionally, we found up-regulation of 1 actin, 2 actin binding protein coding genes [abnormal nuclear anchorage (*anc-1*) and levamisole resistant (*lev-11*)], 3 myosin heavy chain structural genes, 6 *unc* genes and 1 plectin repeat containing gene.

We identified differential regulation of 14 genes related to lipid metabolism and transport. A gene encoding fatty acid desaturase 1 was significantly induced during sedentary stages (stages 3-5) of RKN indicating synthesis of fatty acids required for RKN development. We also observed significant up-regulation of 4 genes encoding lipid transport proteins and 3 genes encoding cytosolic fatty acid binding protein at stage 5 (Fig. 6b). During resistant responses, we observed significant up-regulation of genes encoding FAR protein and cytosolic fatty-acid binding at stage 2 as compared to susceptible response.

Differential regulation of effector genes that suppress plant defense responses

In our study, we have found significant expression of a catalase protein-coding gene at stage 1 and down-regulation at stages 2-5. Also, we observed significant up-regulation of a peroxiredoxin (*PRX2.1*) at stage 3 and superoxide dismutase (*SOD*) at stages 3-5. Apart from

antioxidants, we identified differential expression of 17 genes coding for C-type lectins. Nine of 16 genes were significantly down-regulated during later stages and 5 throughout disease development (Fig. 6b).

A gene encoding 14-3-3 protein was significantly induced at stage 5 (Fig. 5c). Additionally, we observed differential expression of 7 genes coding for oesophageal gland cell secretory proteins (msp), msp1 was significantly induced at stage 3, msp10 at stage 5 whereas msp25, msp30, msp32 and msp37 were significantly suppressed at later stages (Fig. 5c).

In resistance responses, we found significant up-regulation of a gene encoding *MAP-1* protein as compared to susceptible response at stage 2. Additionally, significant up-regulation of 2 *GSTs*, 1 hydroperoxide reductase, 1 aldehyde dehydrogenase, 1 catalase protein, 15 C-type lectins (5 were unique to resistance responses) and 2 autophagy-related proteins was observed.

Expression profiling of a few RKN genes by qRT-PCR

Expression profiles of 6 RKN genes (Table S4) were determined in RKN-infected tomato root tissues at stage 2 (early) and stage 5 (late) of disease development by qRT-PCR. A significant differential expression amongst RKN genes was observed (Fig. S17), which was confirmed by student's t-test at p-value<0.1 and p-value<0.05. The expression of genes encoding EF1, collagen, MAP1, peptidase and C-type lectin was down-regulated at stage 5 as compared to stage 2. Whereas the expression of gene coding for Mj-NULG1a was up-regulated at stage 5 as compared to stage 2.

Discussion

To the best our knowledge, this is the first comprehensive analysis of global gene expression profiles of both tomato and RKN at five stages during susceptible response and two stages during resistance response from *in vivo* RKN-infected tomato roots, under soil-grown conditions. Differentially expressed genes (DEGs) are identified by comparing expression

profiles from infected roots with equivalent developmental stages of uninfected roots. This approach has identified a large set of DEGs along with their temporal regulation during specific stages of disease development. Additionally, we have constructed a model to depict dynamic changes in expression of genes involved in biological processes from both tomato and RKN during susceptible and resistance responses based on the summary of transcriptome data (Fig. 7).

RNASeq data revealed 462 RKN-DEGs during susceptible (Fig. 7a) and 160 RKN-DEGs at stage 2 during resistance responses (Fig. 7b). Here, for the first time, changes in RKN genes expression from *in vivo* infected resistant tomato roots has been presented. Furthermore, RNASeq data revealed 1,827 tomato-DEGs during susceptible (Fig. 7b) and 25 tomato-DEGs during resistance responses (Fig. 7d).

RKNs use mechanical force of the stylet and secrete cell wall degrading or modifying enzymes (CWD/MEs), including endoglucanases, pectate lyases, polygalacturonases, expansins, etc., to macerate plant roots during invasion and migration (Mitchum et al., 2103). Accordingly, we observed activation of RKN genes encoding CWD/MEs, belonging to glycosyl hydrolase (GH) and pectate lyase (PL) families, at stages 1-2 (Fig. 7a) during susceptible responses. As compared to susceptible response, in resistance response the differential expression of 4 (out of 7) genes encoding members of GH family and 2 (out of 5) genes encoding members of PL family were unique to resistance responses (Fig. 7c). The correlation between the reduction in invasion and increased expression along with the different set of RKN CWDEs is noteworthy and needs further investigation. After initiation of feeding cells (stage 2 in our study), expression of genes encoding CWD/MEs are reduced in nematodes and are induced in plants to allow remodelling of cell walls for formation of feeding cells (reviewed in Sobczak et al., 2011). Moreover, up-regulation of tomato genes encoding expansin and glucan endo-beta glucosidase at stage 2 in our study indicates initiation of dynamic changes in plant cell wall architecture (Fig. 7b). However, at later stages (stages 3-5), 53% of the plant genes encoding CWD/MEs (46 out of 86) were down-regulated (Fig. S6), indicating that CWD/MEs are tightly regulated in RKN-

infected tomato roots. By contrast, during resistance responses, lack of differential expression of any of the plant CWD/MEs suggests that these enzymes are not induced in the absence of GC and gall formation. Considering the expression of plant CWD/MEs during both susceptible and resistance responses, it is likely that plant CWD/MEs are largely involved in cell expansion and cell wall restructuring during gall formation and that RKN effectors are involved in modulating their expression during disease development.

In susceptible plants, dramatic morphological changes occur in plant roots leading to a characteristic gall development. During this process, crucial roles of genes encoding TFs from no apical meristem (NAC) and lateral organ boundaries domain-containing (LBD) families have been reported (Portillo et al., 2013; Cabrera et al., 2014). In our study, 5 genes encoding members of NAC domain TF family were specifically down-regulated at stage 3, while LBD4 was up-regulated. Furthermore, 7 novel genes encoding members of root cap protein were down-regulated at stages 3-5 (Fig. S7). This indicates their role in transcriptional reprogramming to control root tip development and lateral root initiation. A number of amino acids are also synthesized in GCs as nutrients for parasitic nematodes. Biochemical assays on amino acids indicate that glutamine is essential for cyst nematode development (Betka *et al.*, 1991). In our study, down-regulation of tomato genes encoding glutamate decarboxylase and tyrosine aminotransferase, which catabolise glutamate and tyrosine, was observed at stages 3-5. This inhibits the break-down of amino acids and allows their availability for RKN development, as was shown in cyst nematodes. With high demand for nutrients transport, we observed differential regulation of tomato genes encoding peptide transporters, nodulin-like sugar transporters, aquaporins, ion transporters and auxin efflux carriers. Furthermore, our study reports for the first time, differential expression of 15 genes encoding MATE efflux family proteins, which are known to play a role in plant growth, development and transport of xenobiotic organic cations (Fig. 7b; Eckardt 2001). In contrast to susceptible responses, no alteration in expression of tomato genes involved in plant cell cycle, cell division, primary or

secondary metabolisms was observed in resistance responses, confirming the cessation of GC formation.

In susceptible plants, feeding RKNs go through transition of larval stages into adults, which is accompanied by the formation of a new cuticle. In our study, 16 cuticle biosynthetic genes were identified and their temporal gene expression patterns corresponding to RKN developmental stages indicated their role as structural proteins in cuticle (Fig. 6a, 7a). Earlier studies on proteases from both animal- and plant-parasitic nematodes have suggested their roles in digestion, embryogenesis, cuticle remodelling and parasitism (references in Haegeman *et al.*, 2012). Furthermore, we observed specific up-regulation of 16 (out of 17) RKN genes encoding ribosomal proteins (not reported previously) during susceptible response, which are known to play role in structural assembly of ribosome. By contrast, absence of feeding cell development in resistant plants leads to starvation-induced stress in nematodes and subsequently cessation of their development. Accordingly, no significant change in expression of genes encoding RKN cuticle collagens was observed in resistant plants. However, up-regulation of RKN genes that regulate actin and myosin filament dynamics was observed, possibly reflecting changes in cytoskeleton and body wall muscles under starvation stress. For example, *unc-87* gene, which is known to stabilize actin filaments for proper functioning of body wall muscles (Yamashiro *et al.*, 2007), was up-regulated at stage 2 (Fig. 7c).

Progress has been made to functionally characterize several RKN genes encoding a wide range of effectors (Mitchum et al., 2013), which have diverse roles during parasitism. For instance, nematode FAR-1 effector is known to interfere with lipid signalling, alteration of cell wall organization and suppression of plant defense responses (Prior *et al.*, 2001; Iberkleid *et al.*, 2015). We found up-regulation of 2 RKN genes encoding FAR at stages 3-5 during susceptible interactions, which can be related to suppression of plant defense responses during later stages of disease development. Another effector gene *Mj-nulg1a*, which is known to target GC nuclei, has been implicated in reducing the parasitism ability of nematode at early stages (2-5 days) of

infection (Lin *et al.*, 2013). In our study, up-regulation of *Mj-nulg1a* gene at later stages (stages 4-5) during susceptible responses suggests that it plays a role in suppression of plant defense responses throughout disease development. Interestingly, during resistance responses, up-regulation of a *FAR* gene and *Mj-nulg1a* gene at stage 2 was also observed (Fig. 7). Since *Mi*-mediated resistance is not complete, their up-regulation during resistance responses might suggest that a few parasitic juveniles (that escaped plant defense responses) attempt to suppress defense responses. A well-characterised RKN effector, CM II was up-regulated at stages 1-2 during susceptible responses, which is in agreement with reported role of CM II during early stages in promoting metabolism of chorismate to prephenate and suppression of SA synthesis (Huang *et al.*, 2005). Another gene encoding a putative RKN avirulence (MAP-1) protein belonging to multigene family and expresses in amphids, has previously been described to play a role during early stages of RKN infections (Semblat *et al.*, 2001; Castagnone-Sereno *et al.*, 2009; Vieira et al., 2011). More recently, all the members of *map-1* gene family from *M. incognita* have been shown to possess conserved similar CLE-like motifs of at least 12 amino acids but the number and arrangements of repeats are different (Rutter et al., 2014b). Here, we report for the first time, expression patterns of *map-1* genes during parasitic stages in both susceptible and resistance responses. We observed that 4 *map-1* genes were up-regulated at stage 2 during resistance (one was unique to resistance response) and were down-regulated at stages 3-5 during susceptible response (one was unique to susceptible response). Based on their structural property and expression patterns, it is likely that they play a role during early stages of infection and may mimic host proteins to modulate plant developmental processes as similar to plant CLE-like peptides (Leasure & He, 2012).

A number of candidate effector genes encode secretory proteins (msp) that are specific to *M. incognita,* but have not yet been annotated (Huang et al., 2003). However, functional roles of *msp16, msp9, msp12, msp18, msp20, msp24, msp33* and *msp40* genes in nematode parasitism have been investigated using gene-silencing approaches (Huang et al., 2006; Xue et al., 2013;

Niu et al., 2016; Shivakumara et al., 2016; Xie et al., 2016). Our study showed for first time that *msp1, msp10, msp25, msp30, msp32* and *msp37* are expressed throughout the parasitic cycle of RKN during susceptible responses (Fig. 7a), also indicating their crucial role in parasitism. Interestingly, up-regulation of *msp37* and *msp32* genes was observed at stage 2 during resistance responses (Fig. 7c) and needs to be further investigated. Additionally, we identified 40 novel RKN-DEGs encoding secretory proteins during susceptible responses based on the presence of signal peptide sequence and absence of trans-membrane domain (Fig. 5a,b). Stage-specific expression profile of these novel RKN genes indicates their potential function in nematode parasitism and/or development.

In resistance responses, up-regulation in expression of tomato genes encoding defensin protein and subtilisin-like protease leading to production of phytoalexins and stress-induced proteolysis was observed. We also found up-regulation of genes involved in activation of signal transduction pathways, including receptor-like kinase and protein phosphatase 2C. However, host defenses are suppressed by parasitic nematodes during susceptible interactions (Favery et al., 2016). In our study, we detected up-regulation of tomato genes involved in polyamines and sterols biosynthesis, and suppression of genes involved in lignin, flavonoids, isoflavonoids and anthocyanins biosynthesis (Fig. 7b) during susceptible responses. Furthermore, up-regulation of 3 genes involved in biosynthetic pathway of spermine and down-regulation of 13 genes encoding ACO indicates suppression of ET biosynthesis (Kumar *et al.*, 1997; Hewezi *et al.*, 2010). In agreement with previous studies, down-regulation of commonly used SA markers (PR-related genes, subtilisin-like proteases and beta-1,3-glucanase) and up-regulation of genes encoding ethylene responsive transcription factors1,2,7,9,10 (ERFs) was observed at stages 4-5 during susceptible response (Fig. 7b). Additionally, genes encoding JAZ proteins (JAZ 1-3) were up-regulated, while a downstream transcription factor gene, MYC2 (myelocytomatosis-related proteins), was down-regulated. This suggests that JAZ proteins are actively involved in suppression of JA-regulated transcription of genes (Chini *et al.*, 2007) during disease

development.

In our study, the components of ET, ABA and SA signalling were differentially regulated during both susceptible and resistance responses. For instance, ABA-responsive genes, *HVA22-like* and *MLP* along with SA-responsive genes methyl carboxylase, were up-regulated at stage 2 in resistance responses and at stages 3-5 in susceptible responses. Interestingly, HVA22-like protein is known to be induced by ABA and acts downstream of GA-Myb TF to suppress GA-mediated apoptosis (Guo & Ho, 2008). The expression pattern of *HVA22* gene during tomato-RKN interactions has not been previously reported. Furthermore, genes encoding ERF10 and ERF2b were up-regulated at stage 2 in resistance responses and at stages 4, 5 in susceptible responses, indicating an active role of ET signalling in plant-nematode interactions. The involvement of ABA-, ET- and SA-mediated defense responses during both susceptible and resistance responses suggest an overlap between biotic and abiotic stress signalling pathways in tomato-RKN interactions (Fig. 7d). Taken together, ABA and ET signalling pathways are induced, whereas SA and JA pathways are suppressed in susceptible interactions (Fig. 7b) while, ABA- and ET-signalling pathways are induced at early stages during resistance interactions.

To evade plant defense responses throughout disease development, RKNs produce an array of antioxidants like catalases, peroxidases, peroxiredoxin, thioredoxins, glutathione-S-transferases and superoxide dismutase (SOD) (Haegeman *et al.*, 2012; Latina, 2015). In our study, a RKN gene encoding catalase was up-regulated at stage 2 during resistance response and down-regulated at stages 2-5 during susceptible responses. Also, we observed up-regulation of 2 genes encoding GST at stage 2 during resistance responses. Significant induction of these antioxidants indicates their role in scavenging host-derived ROS. Additionally, RKN C-type lectins, which are known to suppress the production of ROS, were up-regulated at stage 2 during resistance and down-regulated at stages 3-5 during susceptible responses (Fig. 7a). Furthermore, during resistance responses, increase in the expression of 7 RKN genes encoding peptidases and 2 RKN genes encoding autophagy-related protein at stage 2 (being reported for the first time in this

study), indicates starvation-induced proteolysis of proteins and apoptotic cell death, respectively (Fig. 7c).

In conclusion, this study provides a much deeper and novel insights into the molecular mechanisms involved in plant-nematode interactions. The study has led to identification of a large number of novel and known differentially expressed genes simultaneously from tomato and RKN and their specific modulation during susceptible and/or resistance responses in *in vivo* infected tomato roots under soil-grown conditions. The large repertoire of genes would greatly facilitate basic and applied research on plant-nematode interactions.

Experimental procedures

Plant material and RKN Infection

Two susceptible tomato cultivars used in the study were Pusa Ruby (PR) and Moneymaker (MM). Also, a resistant transgenic tomato MM line containing *Mi* gene (M36) was used. Seeds of the transgenic M36 line were obtained from Prof. Valerie M. Williamson (UC, Davis, USA). Tomato seeds were germinated in trays (36cm x 25cm x 7cm) in sterile soil:solrite (1:4) at 22±2ºC, 16h light/8h dark cycle in greenhouse culture room. Three week old seedlings were transferred to black trays, each having 50 pots (each 4cm in diameter) in soil:sand (1:1). Stocks of *Meloidogyne incognita* were originally obtained from Prof. Uma Rao (IARI, Delhi, India) and were maintained on susceptible tomato and brinjal plants in a greenhouse culture room. Infected roots were collected; egg masses were hand-dissected and kept in sterile water for hatching at room temperature. Five-week old tomato seedlings were inoculated with 1500 freshly hatched J2s per plant and water (control). Whole roots at different days post infection (dpi) were collected with two to five technical replicates, quickly washed with water and then frozen in liquid nitrogen to prevent RNA degradation. The experiment was conducted with two biological replicates. Whole root samples were stored at -80 ºC until RNA isolation.

Disease development stages

Selection of different stages of infection was done independently using acid-fuchsin staining before conducting the main experiments. RKN infection was monitored for 30 days after infection in 'PR' and 7 days after infection in 'M36' by staining the roots with acid fuchsin (Fisher scientific) to determine the exact developmental stages of RKN inside the roots, as described by Byrd et al. 1983. Whole mounts of roots were prepared to count the number of nematodes at each stage for both susceptible and resistance tomato lines under the stereomicroscope (Discovery v.20, Ziess). This study led to selection of five different infected stages in susceptible responses, two stages in resistance responses and a stage 0 (0 dpi/uninfected) (Fig. 1). Since nematode infection is not synchronous tissue from three consecutive infected days were pooled as follows: stage 1 (1,2,3 dpi; invasion of J2s/initiation of feeding sites), stage 2 (5,6,7 dpi; parasitic J2s/formation of feeding sites), stage 3 (13,14,15 dpi; feeding J2s & J3s/expansion of feeding sites), stage 4 (18,19,20 dpi; J4s/maintenance of feeding sites) and stage 5 (26,27,28 dpi; J4s & females/maintenance of feeding sites), to enrich the tissue for that particular stage of nematode infection. In resistance response, we have considered only the first two stages for the study because it has been determined that *Mi-mediated* resistance is an early and rapid response, which is characterized by localized cell death at the site of infection. As a result, the disease does not progress further (Williamson 1998). The approximate count of number of parasitic nematodes inside the infected roots at each stage were as follows: stage 1 susceptible plants had 550 nematodes, while stage 1 resistant plants had 211 nematodes; stage 2 susceptible plants had 680 nematodes, while stage 2 resistant plants had 340 nematodes; stage 3, stage 4 and stage 5 susceptible plants had 430, 700 and 800 nematodes, respectively.

Library preparation and sequencing

Total RNA isolation of uninfected controls and different infected stages from whole roots was carried out independently using Trizol (Molecular Research Centre, Inc., USA) following the

manufacturer's protocol. The quality and quantity of isolated RNA was checked on a 1.2% denaturing agarose gel and nanovue, respectively. For each sample, 4 mg of total RNA was used to construct transcriptome libraries using TruSeq RNA sample preparation kit v2 (Illumina, USA) according to the manufacturer's protocol. cDNA libraries were quantified using Agilent BioAnalyzer 2100 (Agilent technologies, USA) loaded on paired-end (PE) read flow cell (TruSeq v3 kit, Illumina, USA) for first biological replicate and on single-end (SE) read flow cell (TruSeq v3 kit, Illumina, USA) for the second biological replicate. Cluster generation was done on cBot (TruSeq PE and SE cluster kit v3-cBot-HS, Illumina, USA) and sequenced on HiSeq 2000 platform (Illumina, USA).

Transcriptome data analysis

100 bp paired end (PE) reads and single end (SE) reads were demultiplexed using CASAVA tool (Illumina, USA); quality was assessed using FastQC (Andrews, 2010) and filtered using PrinSeq (Schmieder & Edwards, 2011) and Cutadapt (Martin, 2011). A flow summary of transcriptome data analysis is presented in Fig. 8. Filtered reads were aligned independently onto *S. lycopersicum* genome build SL2.50 (Tomato Genome Consortium, 2012) and *M. incognita* WB release 5 (Abad *et al.*, 2008) using TopHat v2.0.14 (Kim *et al.*, 2013) on default parameters. After alignments onto two genomes individually, uniquely mapped reads were further used for quantification by HTSeq (Anders *et al.*, 2015) based on gene annotations. A gene was considered to be expressed and included in the downstream analysis if at least 10 reads were mapped to it aggregated across all the samples. Additionally, tomato genes were annotated using online PANTHER database (Huaiyu et al., 2016) into protein classes and Gene Ontology (GO) with *S. lycopersicum* as reference set. To identify transcription factors, BLASTX was performed against Plant Transcription Factors Database (PlnTFDB; Jin et al., 2014) at e-value of 1e-5 and percentage similarity ≥ 70%.

Prediction of effector molecules

Protein sequences were assessed for secretion by examining for possible signal peptides using SignalP 4.1 (Petersen *et al.*, 2011) and without being possible membrane proteins using TMHMM v.2.0 (Krogh *et al.*, 2001). In addition, we carried out a BLAST search against CDS sequences of known effectors from *Meloidogyne* sp. and cyst nematodes at e-value 1e-5 and percentage similarity ≥ 70%. Furthermore, 'Annotate your protein' tool was used on dbCAN web server for automated annotation of carbohydrate-active enzymes (Yin *et al.*, 2012). Additional data mining was done from the available literature.

Differential gene expression analysis and annotation

For both tomato and RKN, differentially expressed genes (DEGs) were analysed using DESeq2 (Love *et al.*, 2014) in R (v 3.2.3, R Core Team, 2015). Further, to investigate susceptible and resistant tomato responses, the expression of different infected stages was compared to their corresponding uninfected controls to prevent bias due to root development. Cut-off of 0.05 false discovery rate (FDR) and $\log_2$ fold change ≥±2 was used throughout the study (unless stated otherwise). Parametric gene set enrichment analysis on tomato DEGs was performed using AgriGO v 1.2 (Du *et al.*, 2010) with *S. lycopersicum* as reference set. Gene enrichment with a significant threshold of 0.05 after Hochberg false discovery rate correction was used. Functional categorization of DEGs was done using MapMan 3.6.0RC1 (Usadel *et al.*, 2009). In order to highlight specific components and their functions in various pathways, we combined the annotations from gff, GO and MapMan. Redundancy in annotation was checked based on the gene locations on the tomato genome as well as nucleotide and protein sequence similarity.

To investigate RKN responses in susceptible plants, RKN predicted genes from stage 1 were used as a baseline. In order to analyse differences in RKN response to different host plants, RKN (same population of J2) predicted genes from resistant plants were compared to RKN predicted genes from susceptible plants of the same stage. Functional annotation of RKN-DEGs from IPR protein domains was used for GO annotation and KEGG database was used for pathway

analysis. Additionally, we performed BLASTx search against *Meloidogyne* sp. and cyst nematodes proteins retrieved from UniProt database. Furthermore, to improve the annotation, BLASTn search was performed against *M. incognita* stage-specific transcriptome data (http://www6.inra.fr/meloidogyne_incognita), transcript sequences of *M. hapla* (WormBase release 8) and *M. floridensis* (WormBase release 8). BLAST search was done at e-value 1e-5 and percentage similarity ≥ 70%. Redundancy in annotation at amino acid sequence was checked. Figure S18 shows a representative multiple sequence alignment and percentage identity matrix of translated amino acid sequence of genes encoding Pectate lyase 1.

Expression profiling by quantitative PCR (qRT-PCR)

For qRT-PCR, the contaminating DNA was removed by treating 10 micrograms of total RNA with Dnase I enzyme (NEB). The quantity and quality of isolated RNA was checked on 1.2% denaturing agarose gel and nanovue, respectively. Two micrograms of DNase-treated RNA was reverse transcribed using Superscript III (Invitrogen) following the manufacturer's protocol. Quantitative real-time PCR was performed with SYBR-Green technology (Roche) on CFX connect real time system (Biorad Inc., USA). Specific qRT-PCR primers were designed using PrimerQuest tool provided by Integrated DNA Technologies (IDT Inc, USA). Relative fold change was calculated using delta delta ct method.

The RNASeq data was validated for tomato genes using qRT-PCR with the same set of tissue as was used for transcriptome study. Specific primers for 20 tomato genes were designed for validation. All reactions were carried out with two technical replicates and three independent biological replicates.

To assess expression profiles of RKN genes, independent experiments were conducted wherein total RNA from RKN J2 juveniles (approximately 10,000 juveniles), stage 2 knots (around 300 knots) and stage 5 knots (around 100 knots) was extracted using Trizol method. The experiments were conducted using knots to enrich the tissue for nematode stage. Specific primers for 7 RKN

genes were designed and 18S rRNA gene was used as internal control (Papolu et al., 2013). Stage 2 (early stage) was used as control sample and expression of different genes was quantified at stage 5 (late stage). A student's t-test was performed for statistical significance at p-value<0.1 and p-value<0.05. For all the *M. incognita* qRT-PCR experiments, the specificity of the PCR amplification was tested using plant genes as negative controls. The uninfected root tissues and RKN-infected root tissues were used to test the specificity of the amplification and primers that showed amplification in only in the RKN-infected tissue was used for qRT-PCR analysis. All reactions were carried out with two technical replicates and two independent biological replicates.

Acknowledgements

A.K thanks NASF-ICAR, Delhi and DU-R&D grant authorities for funding this research. RNA sequencing was carried out at IGIB, Delhi and NRCPB, Delhi. We also thank Dr. Surekha-Katiyar Agarwal of DU South Campus for her help during transcriptome library preparations. The computing facilities of CBS-DTU and Computerome (both at Technical University of Denmark, Denmark) are gratefully acknowledged. We thank Ravi Shankar and Vandana Chawla (IHBT, Palampur) for initial help in bioinformatics analysis.

Conflict of Interest

Authors have no conflict of interest to declare.

References

Abad, P., Gouzy, J., Aury, J., Castagnone-Sereno, P., Danchin, E., Deleury, E., Perfus-Barbeoch, L., Anthouard, V., Artiguenave, F., Blok, V.C., Caillaud, M.C., Coutinho, P.M., Dasilva, C., Luca, F., Deau, F., Esquibet, M., Flutre, T., Goldstone, J.V., Hamamouch, N., Hewezi, T., Jaillon, O., Jubin, C., Leonetti, P., Magliano, M., Maier, T.R., Markov, G.V., McVeigh, P., Pesole, G., Poulain, J., Robinson-Rechavi, M., Sallet, E., Ségurens, B.,

Steinbach, D., Tytgat, T., Ugarte, E., Ghelder, C., Veronico, P., Baum, T.J., Blaxter, M., Bleve-Zacheo, T., Davis, E.L., Ewbank, J.J., Favery, B., Grenier, E., Henrissat, B., Jones, J.T., Laudet, V., Maule, A.G., Quesneville, H., Rosso, M-N., Schiex, T., Smant, G., Weissenbach, J., and Wincker, P. (2008) Genome sequence of the metazoan plant-parasitic nematode *Meloidogyne incognita*. *Nat. Biotechnol.* **26,** 909-915.

Abad, P. and Williamson, V.M. (2010) Plant Nematode Interaction: A Sophisticated Dialogue. In Advances in Botanical research Volume 53 (Kader, J.C., Delseny, M., eds), pp. 147-192. Elsevier.

Anders, S., Pyl, P.T. and Huber, W. (2015) HTSeq--A python framework to work with high-throughput sequencing data. *Bioinformatics* **31**(2), 166-169.

Andrews, S. (2010) FastQC: a quality control tool for high throughput sequence data. Available online at: http://www.bioinformatics.babraham.ac.uk/projects/fastqc.

Bagnaresi, P., Sala, T., Irdani, T., Scotto, C., Lamontanara, A., Beretta, M., Rotino, G.L., Sestili, S., Cattivelli, L. and Sabatini, E. (2013) *Solanum torvum* responses to the root-knot nematode *Meloidogyne incognita. BMC Genomics* **14**, 540.

Barcala, M., Garcia, A., Cabrera, J., Casson, S., Lindsey, K., Favery, B., García-Casado, G., Solano, R., Fenoll, C. and Escobar, C. (2010) Early transcriptomic events in microdissected *Arabidopsis* nematode-induced giant cells. *Plant J.* **61**, 698-712.

Bar-Or, C., Kapulnik, Y. and Koltai, H. (2005) A broad characterization of the transcriptional profile of the compatible tomato response to the plant parasitic root knot nematode *Meloidogyne javanica*. *Eur. J. Plant Pathol.* **111**, 181-192.

Bellafiore, S., Shen, Z., Rosso, M.N., Abad, P., Shih, P. and Briggs, S.P. (2008) Direct identification of the *Meloidogyne incognita* secretome reveals proteins with host cell reprogramming potential. *PLoS Pathogens* **4**(10), e1000192.

Beneventi, M.A., da, Silva, Jr, O.B., de, Sá, M.E.L., Firmino, A.A.P., de, Amorim, R.M.S., Albuquerque, E.V.S., da, Silva, M.C.M., da, Silva, J.P., Campos, M.A., Lopes, M.J.C., Togawa, R.C., Pappas, Jr., G.J. and de, Sa, M.F.G. (2013) Transcription profile of soybean-root-knot nematode interaction reveals a key role of phythormones in the resistance reaction. *BMC Genomics* **14**,322.

Betka, M., Grundler, F. and Wyss, U. (1991) Influence of changes in the nurse cell system (syncytium) on the development of the cyst nematode *Heterodera schachtii* – single amino acids. *Phytopathol.* **81**(1), 75-79.

Bhattarai, K.K., Xie, Q.G., Mantelin, S., Bishnoi, U., Girke, T., Navarre, D.A. and Kaloshian, I. (2008) Tomato susceptibility to root-knot nematodes requires an intact jasmonic acid signalling pathway. *Mol. Plant Microbe Interact.* **21**(9), 1205-1214.

Branch, C., Hwang, C.F., Navarre, D.A. and Williamson, V.M. (2004) Salicylic acid is part of the *Mi-1*-mediated defense response to root-knot nematode in tomato. *Mol. Plant Microbe Interact.* **17**(4), 351-356.

Byrd, D.W., Kirkpatrick, T. and Barker K.R. (1983) An improved technique for clearing and staining plant tissues for detection of nematodes. *Journal of Nematology.* **15**(1), 142-143.

Cabrera, J., Diaz-Manzano, F.E., Sanchez, M., Rosso, M.N., Melillo, T., Goh, T., Fukaki, H., Cabello, S., Hofmann, J., Fenoll, C. and Escobar, C. (2014) A role for *LATERAL ORGAN BOUNDARIES-DOMAIN 16* during the interaction *Arabidopsis-Meloidogyne* spp. provides a molecular link between lateral root and root-knot nematode feeding site development. *New Phytol.* **203**, 632-645.

Castagnone-Sereno, P., Semblat, J.P. and Castagnone, C. (2009) Modular architecture and evolution of the *map*-1 gene family in the root-knot nematode *Meloidogyne incognita*. *Mol. Genet. Genomics* **282**, 547-554**.**

Chini, A., Fonseca, S., Fernandez, G., Adie, B., Chico, J.M., Lorenzo, O., Garcia-Casado, G., Lopez-Vidriero, I., Lozano, F.M., Ponce, M.R., Micol, J.L. and Solano, R. (2007) The JAZ family of repressors is the missing link in jasmonate signalling. *Nature* **448**, 666-671.

de, Ilarduya, O.M., Moore, A.E. and Kaloshian, I. (2001) The tomato *Rme1* locus is required for *Mi-1*-mediated resistance to root-knot nematodes and the potato aphid. *Plant J.* **27**(5), 417-425.

Du, Z., Zhou, X., Ling, Y., Zhang, Z. and Su, Z. (2010) AgriGO: A GO analysis toolkit for the agricultural community. *Nucleic Acids Res.* **38**, *64-70.*

Eckardt, N.A. (2001) Move it on out with MATEs. *The Plant Cell*. **13**, 1477-1480.

Favery, B., Quentin, M., Jaubert-Possamai, S. and Abad, P. (2016) Gall-forming root-knot nematodes hijack key plant cellular functions to induce multinucleate and hypertrophied feeding cells. *J. Insect Physiol.* **84**, 60-69.

Fuller, V.L., Lilley, C.J., Atkinson, H.J. and Urwin, P.E. (2007) Differential gene expression in *Arabidopsis* following infection by plant-parasitic nematodes *Meloidogyne incognita* and *Heterodera schachtii*. *Mol. Plant Pathol.* **8**, 595-609.

Guo, W.J. and Ho, T.H.D. (2008) An abscisic acid-induced protein, HVA22, inhibits gibberellin-mediated programmed cell death in cereal aleurone cells. *Plant Physiol.* **147**, 1710-1722.

Haegeman, A., Bauters, L., Kyndt, T., Rahman, M.M. and Gheysen, G. (2013) Identification of candidate effector genes in the transcriptome of the rice root knot nematode *Meloidogyne graminicola*. *Mol. Plant Pathol.* **14**(4), 379-390.

Haegeman, A., Mantelin, S., Jones, J.T. and Gheysen, G. (2012) Functional roles of effectors of plant-parasitic nematodes. *Gene* **492**(1), 19-31.

Hammes, U.Z., Schachtman, D.P., Berg, R.H., Nielsen, E., Koch, W., McIntyre, L.M. and Taylor, C.G. (2005) Nematode-induced changes of transporter gene expression in *Arabidopsis* roots. *Mol. Plant Microbe Interact.* **18**, 1247-1257.

Hewezi, T., Howe, P.J., Maier, T.R., Hussey, R.S., Mitchum, M.G., Davis, E.L. and Baum, T.J. (2010) Arabidopsis spermidine synthase is targeted by an effector protein of the cyst nematode *Heterodera schachtii*. *Plant Physiol.* **152**, 968-984.

Huaiyu, M.I., Poudel, S., Casagrande, A.M.J.T. and Thomas, P.D. (2016) PANTHER version 10: expanded protein families and functions, and analysis tools. *Nucleic Acids Res.* doi: 10.1093/nar/gkv1194.

Huang, G., Dong, R., Allen, R., Davis, E.L., Baum, T.J. and Hussey, R.S. (2005) Two chorismate mutase genes from the root-knot nematode *Meloidogyne incognita*. *Mol. Plant Pathol.* **6**, 23–30.

Huang, G., Dong, R., Allen, R., Davis, E.L., Baum, T.J. and Hussey, R.S. (2006) A root-knot nematode secretory peptidefunctions as a ligand for a plant transcription factor. *Mol. Plant Microbe Interact.* **19**, 463-470.

Huang, G., Gao, B., Maier, T., Allen, R., Davis, E.L., Baum, T.J. and Hussey, R.S. (2003) A profile of putative parasitism genes expressed in the oesophageal gland cells of the root-knot nematode *Meloidogyne incognita*. *Mol. Plant Microbe Interact.* **16**, 376-381.

Hwang, C.F. and Williamson, V.M. (2003) Leucine-rich repeat-mediated intramolecular interactions in nematode recognition and cell death signalling by the tomato resistance protein Mi. *Plant J.* **34**, 585-593.

Iberkleid, I., Sela, N. and Miyara, S.B. (2015) *Meloidogyne javanica* fatty acid-and retinol-binding protein (Mj-FAR-1) regulates expression of lipid-, cell wall-, stress- and phenylpropanoid-related genes during nematode infection of tomato. *BMC Genomics* **16**, 272.

Ibrahim, H.M.M., Hosseini, P., Alkharouf, N.W., Hussein, E.H.A., El-Din, A.E.K.Y.G., Aly, M.A.M. and Matthews, B.F. (2011) Analysis of gene expression in soybean (*Glycine max*) roots in response to the root-knot nematode *Meloidogyne incognita* using microarrays and KEGG pathways. *BMC Genomics* **12**, 220.

Jammes, F., Lecomte, P., de, Almeida-Engler, J., Bitton, F., Martin-Magniette, M.L., Renou, J.P., Abad, P. and Favery, B. (2005) Genome-wide expression profiling of the host response to root-knot nematode infection in *Arabidopsis*. *Plant J.* **44**, 447-458.

Jaouannet, M., Magliano, M., Arguel, M.J., Gourgues, M., Evangelisti, E., Abad, P. and Rosso, M.N. (2013) The root-knot nematode calreticulin Mi-CRT is a key effector in plant defense suppression. *Mol. Plant Microbe Interact.* **26**, 97–105.

Jaubert, S., Milac, A.L., Petrescu, A.J., de, Almeida-Engler, J., Abad, P. and Rosso, M.N. (2005) In planta secretion of a calreticulin by migratory and sedentary stages of root-knot nematode. *Mol. Plant Microbe Interact.* **18**, 1277–1284.

Ji, H., Gheysen, G., Denil, S., Lindsey, K., Topping, J.F., Nahar, K., Haegeman, A., de, Vos, W.H., Trooskens, G., Criekinge, W.V., Meyer, T.M. and Kyndt, T. (2013) Transcriptional analysis through RNA sequencing of giant cells induced by *Meloidogyne graminicola* in rice roots. *J. Exp. Bot.* **64**, 3885-3898.

Jin, J.P., Zhang, H., Kong, L., Gao, G. and Luo, J.C. (2014) PlantTFDB 3.0: a portal for the functional and evolutionary study of plant transcription factors. *Nucleic Acids Res.* **42**(D1), D1182-D1187.

Jones, J.D.G. and Dangl, J.L. (2006) The plant immune system. *Nature* **244**, 323–329.

Kim, D., Pertea, G., Trapnell, C., Pimentel, H., Kelley, R., Salzberg, S.L. (2013) TopHat2: Accurate alignment of transcriptomes in the presence of insertions, deletions and gene fusions. *Genome Biol.* **14**(4), R36.

Krogh, A., Larsson, B., Heijne, G. and Sonnhammer, E.L.L. (2001) Predicting transmembrane protein topology with a hidden Markov model: application to complete genomes. *J. Mol. Biol.* **305**, 567-580.

Kumar, A., Altabella, T., Taylor, M.A. and Tiburcio. (1997) Recent advances in polyamine research. *Trends in Plant Science* **2**(4), 124-130.

Kyndt, T., Denil, S., Haegeman, A., Trooskens, G., Bauters, L., Van, Criekinge, W., De, Meyer, T. and Gheysen, G. (2012) Transcriptional reprogramming by root knot and migratory nematode infection in rice. *New Phytol.* **196**, 887–900.

Latina, R. (2015) *Functional analysis of Meloidogyne graminicola C-type lectins and their role in the nematode-rice interaction.* Master's thesis, University of Ghent, Ghent, Belgium.

Leasure, C.D. and He, Z.H. (2012) *CLE* and *RGF* family peptide hormone signalling in plant development. *Mol. Plant* **5**(6), 1173-1175.

Li, Q., Xie, Q.G., Smith-Becker, J., Navarre, D.A. and Kaloshian, I. (2006) *Mi-1*-mediated aphid resistance involves salicylic acid and mitogen-activated protein kinase signalling cascades. *Mol. Plant Microbe Interact.* **19**, 655-664.

Lin, B., Zhuo, K., Wu, P., Cui, R., Zhang, L.H. and Liao, J. (2013) A novel effector protein, MJ-NULG1a, targeted to giant cell nuclei plays a role in *Meloidogyne javanica* parasitism. *Mol. Plant Microbe Interact.* **26**, 55-66.

Love, M.I., Huber, W. and Anders, S. (2014) Moderated estimation of fold change and dispersion for RNA-Seq data with DESeq2. *Genome Biol.* **15**(12), 550.

Manosalva, P., Manohar, M., von, Reuss, S.H., Chen, S., Koch, A., Kaplan, F., Choe, A., Micikas, R.J., Wang, X., Kogel, K.H., Sternberg, P.W., Williamson, V.M., Schroeder, F.C. and Klessig, D.F. (2015) Conserved nematode signalling molecules elicit plant defenses and

pathogen resistance. *Nat. Commun.* **6**, 7795 doi: 10.1038/ncomms8795.

Mantelin, S., Bhattarai, K.K., Jhaveri, T.Z. and Kaloshian, I. (2013) *Mi-1*-mediated resistance to *Meloidogyne incognita* in tomato may not rely on ethylene but hormone perception through ETR3 participates in limiting nematode infection in a susceptible host. *PLoS ONE* **8**(5), e63281.

Martin M. (2011) Cutadapt removes adapter sequences from high-throughput sequencing reads. *EMBnet.journal* **17**, 10-12.

Milligan, S.B., Bodeau, J., Yaghoobi, J., Kaloshian, I., Zabel, P. and Williamson, V.M. (1998) The root knot nematode resistance gene *Mi* from tomato is a member of the leucine zipper, nucleotide binding, leucine-rich repeat family of plant genes. *Plant Cell* **10**, 1307-1319.

Mitchum, M.G., Hussey, R.S., Baum, T.J., Wang, X., Elling, A.A., Wubben, M. and Davis, E.L. (2013) Nematode effector proteins: an emerging paradigm of parasitism. *New Phytol.* **199**, 879-894.

Molinari, S., Fanelli, E. and Leonetti, P. (2013) Expression of tomato SA-responsive pathogenesis-related genes in *Mi-1*-mediated and SA-induced resistance to root-knot nematodes. *Mol. Plant Pathol.* **15**(3), 255-264.

Niu, J.H., Liu, P., Liu, Q., Chen, C., Guo, Q., Yin, J., Yang, G. and Jian, H. (2016) Msp40 effector of root-knot nematode manipulates plant immunity to facilitate parasitism. *Sci. Rep.* **6**, 19443.

Papolu, P.K., Gantasala, N.P., Kamaraju, D., Banakar, P., Sreevathsa, R. and Rao U (2013) Utility of host delivered RNAi of two FMRF amide like peptides, *flp-14* and *flp-18*, for the management of root-knot nematode, *Meloidogyne incognita*. *PLoS ONE* **8**(11), e80603.

Petersen, T.N., Brunak, S., Heijne, G. and Nielsen, H. (2011) SignalP 4.0: Discriminating

signal peptides from transmembrane regions. *Nature Methods* **8**, 785-786.

Portillo, M., Cabrera, J., Lindsey, K., Topping, J., Andres, M.F., Emiliozzi, M., Oliveros, J. C., Gracia-Casado, G., Solano, R., Koltai, H., Resnick, N. and Escobar, C. (2013) Distinct and conserved transcriptomic changes during nematode-induced giant cell development in tomato compared with *Arabidopsis*: a functional role for gene repression. *New Phytol.* **197**, 1276e1290.

Postnikova, O.A., Hult, M., Shao, J., Skantar, A. and Nemchinov, L.G. (2015) Transcriptome analysis of resistant and susceptible alfalfa cultivars infected with root-knot nematode *Meloidogyne incognita*. *PLoS ONE* **10**(2), e0118269.

Prior, A.E., Jones, J.T., Blok, V.C., Beauchamp, J., McDermott, L., Cooper, A. and Kennedy, M.W. (2001) A surface-associated retinol- and fatty acid-binding protein (Gp-FAR-1) from the potato cyst nematode *Globodera pallida*: lipid binding activities, structural analysis and expression pattern. *Biochem. J.* **356**, 387-394.

R Core Team. (2015) R: A language and environment for statistical computing. R Foundation for Statistical Computing, Vienna, Austria. Available online at: https://www.R-project.org.

Rutter, W.B., Hewezi, T., Abubucker, S., Maier, T.R., Huang, G., Mitreva, M., Hussey, R.S. and Baum, T.J. (2014a) Mining novel effector proteins from the oesophageal gland cells of *Meloidogyne incognita*. *Mol. Plant Microbe Interact.* **27**(9), 965–974.

Rutter, W.B., Hewezi, T., Maier, T.R., Mitchum, M.G., Davis, E.L., Hussey, R.S. and Baum, T.J. (2014b) Members of the *Meloidogyne* avirulence protein family contain multiple plant ligand-like motifs. *Nematology* **104**, 875-885.

Santini, L., Munhoz, C.F., Bonfim, Jr., M.F., Brandão, M.M., Inomoto, M.M. and Vieira, M.L.C. (2016) Host transcriptional profiling at early and later stages of the compatible interaction between *Phaseolus vulgaris* and *Meloidogyne incognita. Nematology* **106**(3), 282-

294.

Schaff, J.E., Nielsen, D.M., Smith, C.P., Scholl, E.H. and Bird, D.M. (2007) Comprehensive transcriptome profiling in tomato reveals a role for glycosyltransferase in *Mi*-mediated nematode resistance. *Plant Physiol.* **144**, 1079-1092.

Schmieder, R. and Edwards, R. (2011) Quality control and preprocessing of metagenomic datasets. *Bioinformatics* **27**, 863-864.

Semblat, J.P., Rosso, M.N., Hussey, R.S., Abad, P. and Castagnone-Sereno, P. (2001) Molecular cloning of a cDNA encoding an amphid-secreted putative avirulence protein from the root-knot nematode *Meloidogyne incognita*. *Mol. Plant Microbe Interact.* **14**, 72-79.

Shivakumara, T.N., Papolu, P.K., Dutta, T.K., Kamaraju, D., Chaudhary, S. and Rao, U. (2016) RNAi-induced silencing of an effector confers transcriptional oscillation in another group of effectors in the root-knot nematode, *Meloidogyne incognita*. *Nematology* **00**, 1-14.

Shukla, N., Kaur, P. and Kumar, A. (2016) Molecular aspects of plant-nematode interactions. *Ind J Plant Physiol.* **21**(4), 477-488. DOI 10.1007/s40502-016-0263-y.

Sobczak, M., Fudali, S. and Wieczorek, K. (2011) Cell wall modifications induced by nematodes. In Genomics and Molecular Genetics of Plant-Nematode Interactions (Jones, J., Gheysen, G. and Fenoll C., eds), pp. 395-422. Netherlands, Springer.

Stotz, H.U., Spence, B. and Wang, Y. (2009) A defensin from tomato with dual function in defense and development. *Plant Mol. Biol.* **71**, 131-143.

Tomato Genome Consortium. (2012) The tomato genome sequence provides insights into fleshy fruit evolution. *Nature* **485**, 635-641.

Trudgill, D.L. and Block, V.C. (2001) Apomictic, polyphagous root-knot nematodes, exceptionally successful and damaging biotrophic root pathogens. *Annu. Rev. Phytopathol.* **39**,

53-77.

Truong, N.M., Nguyen, C.N., Abad, P., Quentin, M. and Favery, B. (2015) Function of root-knot nematode effectors and their targets in plant parasitism. In Advances in Botanical research Volume 73 (Escobar, C., Fenoll, C., eds), pp. 293-324. Elsevier.

Usadel, B., Poree, F., Nagel, A., Lohse, M., Czedil-Eysenberg, A. and Stitt M. (2009) A guide to using MapMan to visualize and compare omics data in plants: a case study in the crop species, Maize. *Plant Cell Environ.* **32**, 1211-1229.

Vieira, P., Danchin, E.G., Neveu, C., Crozat, C., Jaubert, S., Hussey, R.S., Engler, G., Abad, P., de Almeida-Engler, J., Castagnone-Sereno, P. and Rosso, M.N. (2011) The plant apoplasm is an important recipient compartment for nematode secreted proteins. J. Exp. Bot. **62**, 1241-1253.

Williamson, V.M. (1998) Root-knot nematode resistance genes in tomato and their potential for future use. *Annu. Rev. Phytopathol.* **36**, 277-293.

Williamson, V.M. and Hussey, R.S. (1996) Nematode pathogenesis and resistance in plants. *Plant Cell* **8**, 1735-1745.

Williamson, V.M. and Kumar, A. (2006) Nematode resistance in plants: the battle underground. *Trends Genet.* **22**(7), 396-403.

Xie, J., Li, S., Mo, C., Wang, G., Xiao, X. and Xiao, Y. (2016) A novel *Meloidogyne incognita* effector Misp12 suppresses plant defense response at later stages of nematode parasitism. *Front. Plant Sci.* **7**, 964.

Xue, B., Hamamouch, N., Li, C., Huang, G. and Hussey, R.S. (2013) The 8D05 parasitism gene of *Meloidogyne incognita* is required for successful infection of host roots. *Phytopathology* **103**, 175-181.

Yamashiro, S., Gimona, M. and Ono, S. (2007) UNC-87, a calponin repeat protein in *C. elegans*, antagonizes ADF/cofilin-mediated actin filament dynamics. *J. Cell Sci.* **120**, 3022-3033.

Yin, Y., Mao, X., Yang, J.C., Chen, X., Mao, F. and Xu, T. (2012) A web resource for automated carbohydrate-active enzyme annotation. *Nucleic Acids Res.* **40**(Web Server issue), W445-51.

Author contributions

A.K conceived the project and designed the experiments. P.K and N.S set up the RKN infection in tomatoes and performed staining experiments. N.S performed the wet experiments and the transcriptomic data analysis. All bioinformatics work was done under the supervision of R.Y and R.G and R.Y also carried out some of the bioinformatics analysis. N.S, R.Y and A.K wrote the manuscript and all the authors made changes to the initial and revised manuscripts and approved the final version.

Supporting Information

Fig. S1 Heatmap showing the correlation among various susceptible samples and replicates based on global expression profiles.

Fig. S2 Gene ontology (GO) annotation of significant tomato-DEGs detected during susceptible response at various stages of disease development.

Fig. S3 Distribution of significant tomato-DEGs detected during susceptible response into various protein classes.

Fig. S4 Distribution of significant tomato-DEGs into various protein classes detected at stage 2 during (a) susceptible and (b) resistant responses.

Fig. S5 Gene set enrichment analysis of molecular functions for tomato-DEGs detected during susceptible response at (a) stage 4 and (b) stage 5.

Fig. S6 Schematic representation of gene expression patterns of significant tomato-DEGs involved in plant cell wall architecture detected during susceptible response.

Fig. S7 Schematic representation of gene expression patterns of significant tomato-DEGs involved in plant root development detected during susceptible response.

Fig. S8 Schematic representation of gene expression patterns of significant tomato-DEGs involved in (a) primary sugar metabolism (b) amino acid metabolism (c) lipid and fatty acid metabolism and (d) other primary metabolism categories detected during susceptible response.

Fig. S9 Schematic representation of gene expression patterns of significantly differentially expressed (a) sugar transporter genes, (b) lipid transporter genes, (c) aquaporin transporter genes, (d) amino acid and peptide transporter genes, (e) Multidrug and toxic compound extrusion (MATE) transporter family genes and (f) various inorganic ion transporter genes in tomato roots detected during susceptible response.

Fig. S10 Schematic representation of gene expression patterns (left) of tomato-DEGs involved in (a) isoprenoids and (b) polyamines biosynthetic pathways (right). Pathways showing DEGs (in red) and end products of pathways (in green) during susceptible response.

Fig. S11 Schematic representation of gene expression patterns of significant tomato-DEGs from (a) auxin, cytokinin and brassinosteroid responsive and (b) ABA responsive categories detected during susceptible response.

Fig. S12 Heatmap of Log2FoldChanges of significantly differentially expressed ethylene responsive transcription factors detected at various stages of disease development in susceptible tomato roots.

Fig. S13 Schematic representation of gene expression patterns of tomato-DEGs involved in (a) jasmonic acid and (b) salicylic acid biosynthesis and signalling (c) oxidative stress-related genes detected during susceptible response.

Fig. S14 Scatter plot showing correlation between RNASeq and qRT-PCR expression profiles.

Fig. S15 Heatmap showing global gene expression profile of total RKN genes identified from infected tomato roots at five different infection time intervals.

Fig. S16 (a) Distribution of significant RKN-DEGs into top 30 IPR protein domains detected at different stages of infection from susceptible tomato roots as compared to stage 1. (b) Distribution of significant RKN-DEGs into top 30 KEGG pathways detected at different stages of infection from susceptible tomato roots as compared to stage 1.

Fig. S17 Expression profiles of RKN genes determined by quantitative reverse transcription-polymerase chain reaction (qRT-PCR) analysis.

Fig. S18 (a) Multiple sequence alignment of translated amino acid sequences of RKN genes encoding pectate lyase 1 and (b) Percentage identity matrix of translated amino acid sequences

of RKN genes encoding pectate lyase 1.

Table S1 Statistics of raw reads and quality filtering of transcriptome libraries.

Table S2 Significant differentially expressed tomato genes detected at various stages of disease development during susceptible responses.

Table S3 Significant differentially expressed tomato genes detected at stage 2 during resistance response.

Table S4 Primer sequences of tomato genes and RKN genes used for quantitative PCR (qRT-PCR) expression analysis.

Table S5 Significant differentially expressed RKN genes detected at various stages of disease development during susceptible responses.

Table S6 Significant differentially expressed RKN genes detected at stage 2 during resistance response.

Figure and Table legends

Table 1. Statistics of good quality reads mapped onto tomato and nematode reference genomes.

Fig. 1 *Meloidogyne incognita* life cycle in susceptible tomato cultivar Pusa Ruby (PR) roots. Whole mounts (10 μm) of acid fuchsin stained roots with parasitic nematodes (black arrows) at different stages (Stages 1-5) inside the roots are presented. dpi, days post infection; EM, egg masses; J2s, second-stage juveniles.

Fig. 2 (a) Distribution of significant differentially expressed genes (DEGs) in tomato at different stages during susceptible response. (b) Comparative expression profile of tomato-DEGs detected during susceptible (PR) and resistance responses (M36) at stage 2. Differential expression was calculated with respect to the corresponding uninfected controls. Each row of heatmap represents a gene and each column represents stage of disease development. Color key is given on top-left corner of the figure. **(c and d) Quantitative reverse transcription-polymerase chain reaction (qRT-PCR) validation of RNASeq data for tomato genes, receptor-like kinase gene and glucan endo-1,3-beta glucosidase gene during resistance and susceptible responses, respectively.** Y axes represent relative fold change (calculated using delta delta ct method) in gene expression at various stages as compared to corresponding uninfected controls. Data are representative of two technical replicates and three independent biological replicates. Bars indicate standard errors. B1, biological replicate 1; B2, biological replicate 2; UI, uninfected; I, infected; M36, transgenic resistant to RKN; PR, susceptible to RKN.

Fig. 3. Schematic representation of gene expression patterns of subsets of tomato DEGs involved in (a) plant cell wall architecture, (b) development, (c) primary metabolism and (d) transporter genes in susceptible response. The heatmap represents only a subset of genes from each category, consult supplementary data for expression of all DEGs involved in each

category. Each row represents a gene and each column represents stage of disease development. Labels on the right side of heatmap states gene id then category to which it belongs followed by annotation. Color key is given on top-left corner of heatmap.

Fig. 4. Schematic representation of gene expression patterns (left) of tomato-DEGs involved in phenylpropanoid biosynthetic pathway (right). Pathway showing DEGs (in red) and end products of pathways (in green) during susceptible response. In heatmap, each row represent a gene and each column represents stage of disease development. Labels on right side of heatmap states gene id followed by annotation. Color key is given on top-left corner of figure. 4CL, 4-hydroxycinnamoylCoA ligase; CAD, cinnamyl alcohol dehydrogenase; CCoAMT, caffeoylCoA-O-methyltransferase; HCT, Hydroxycinnamoyl shikimate/quinate hydroxycinnamoyl transferase; HCoA, Hydroxycinnamoyl Co A; PAL, phenylalanine ammonia lyase.

Fig. 5(a) Distribution of significant RKN differentially expressed genes (DEGs) detected at different stages of infection as compared to stage 1 during susceptible response. (b) Workflow summary of bioinformatic strategy used to identify RKN candidate effector genes. (c) Schematic representation of gene expression patterns of RKN-DEGs reported to be involved in parasitism during susceptible response. Each row represents a gene and each column represents stage of disease development. Labels on right side states gene id followed by annotation. Color key is given on top-left corner of figure.

Fig. 6. Schematic representation of gene expression patterns of RKN-DEGs involved in (a) cell wall degradation and peptidase-encoding (b) development, metabolism and nematode immunity, detected during susceptible response. Each row represents a gene and each column represents stage of disease development. Labels on right side of heatmap states gene id followed by annotation. Color key is given on top-left corner of figure.

Fig. 7. A model that depicts complex changes in the biochemical processes in both tomato

and RKN during susceptible and resistant interactions based on the summary of transcriptome data. **(a)** Changes in expression of RKN genes during susceptible responses. **(b)** Changes in expression of tomato genes during susceptible responses. **(c)** Changes in expression of RKN genes during resistance responses. **(d)** Changes in expression of tomato genes during resistance responses. The up-arrow head indicates up-regulated genes; down-arrow head indicates down-regulated genes and numerical sub-script in the arrowhead indicates specific stages where the expression was observed. Host metabolic process that are modulated upon RKN-infection are highlighted in colored circles. ABA, abscisic acid; ACO, 1-aminocyclopropane-1-carboxylic acid oxidase; Avr, avirulence protein; CAD, cinnamyl alcohol dehydrogenase; CM II, chorismate mutase type-II; ERF, ethylene responsive transcription factor; FAR, nematode fatty-acid retinol binding protein; GA, gibbrellins; LBD, lateral organ body domain containing transcription factor; LOX, lipoxygenase; MAP-1, *Meloidogyne* avirulence protein; NAC TF, no apical meristem containing transcription factor; MAP65-1a, microtubule associated protein 65-1a; pat, paralysed arrest two-fold; PR1, pathogenesis-related protein 1; SA, salicylic acid; SOD, superoxide dismutase; unc, uncoordinated; Wox4, WUS homeobox containing gene.

Fig. 8. Workflow summary used for transcriptome data analysis.

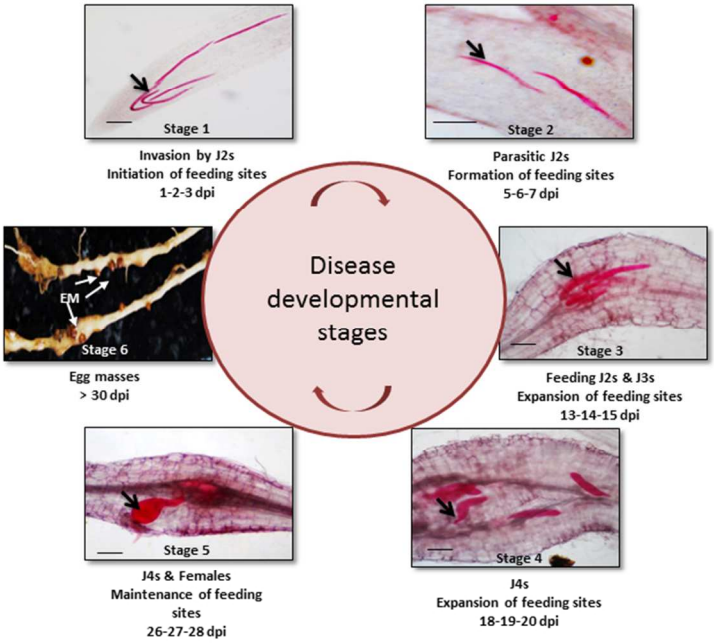

Fig. 1 *Meloidogyne incognita* life cycle in susceptible tomato cultivar Pusa Ruby (PR) roots. Whole mounts (10 µm) of acid fuchsin stained roots with parasitic nematodes (black arrow) at different stages (Stages 1-5) inside the roots are presented. dpi, days post infection; EM, egg masses; J2s, J3s and J4s, juveniles in the second, third and forth stages of development.

190x275mm (96 x 96 DPI)

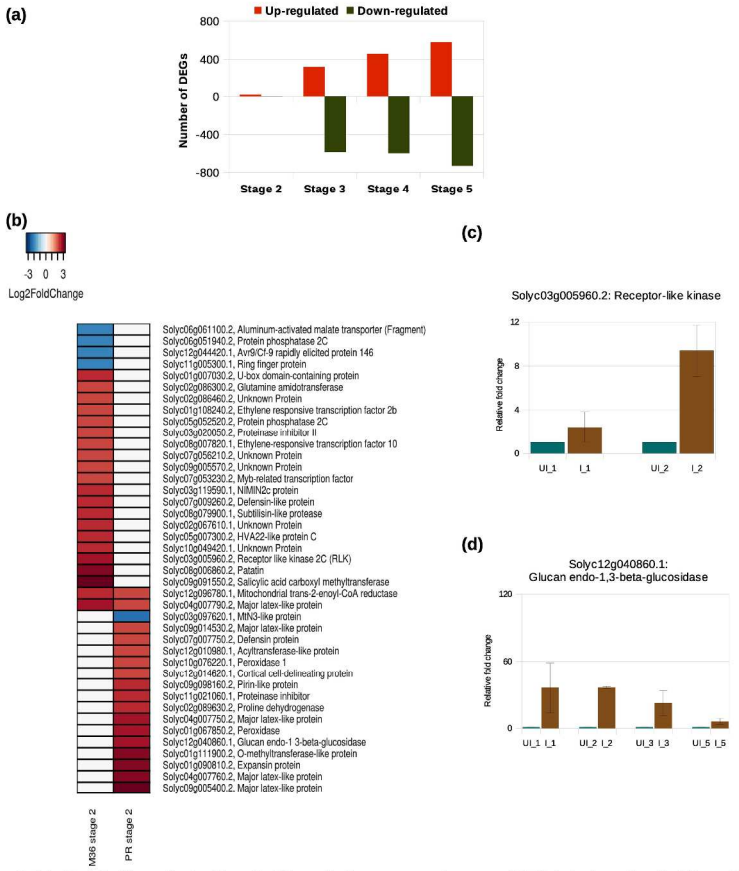

Fig. 2 (a) Distribution of significant differentially expressed genes (DEGs) in tomato at different stages during susceptible response. (b) Comparative expression profile of tomato-DEGs detected during susceptible (PR) and resistance responses (M36) at stage 2. Differential expression was calculated with respect to the corresponding uninfected controls. Each row of heatmap represents a gene and each column represents stage of disease development. Color key is given on top-left corner of the figure. **(c and d) Quantitative reverse transcription-polymerase chain reaction (qRT-PCR) validation of RNASeq data for tomato genes, receptor-like kinase gene and glucan endo-1,3-beta glucosidase gene during resistance and susceptible responses, respectively.** Y axes represent relative fold change (calculated using delta delta ct method) in gene expression at various stages as compared to corresponding uninfected controls. Data are representative of two technical replicates and three independent biological replicates. Bars indicate standard errors. B1, biological replicate 1; B2, biological replicate 2; UI, uninfected; I, infected; M36, transgenic resistant to RKN; PR, susceptible to RKN.

297x420mm (300 x 300 DPI)

Fig. 3. Schematic representation of gene expression patterns of subsets of tomato DEGs involved in (a) plant cell wall architecture, (b) development, (c) primary metabolism and (d) transporter genes in susceptible response. The heatmap represents only a subset of genes from each category, consult supplementary data for expression of all DEGs involved in each category. Each row represents a gene and each column represents stage of disease development. Labels on the right side of heatmap states gene id then category to which it belongs followed by annotation. Color key is given on top-left corner of heatmap.

297x420mm (300 x 300 DPI)

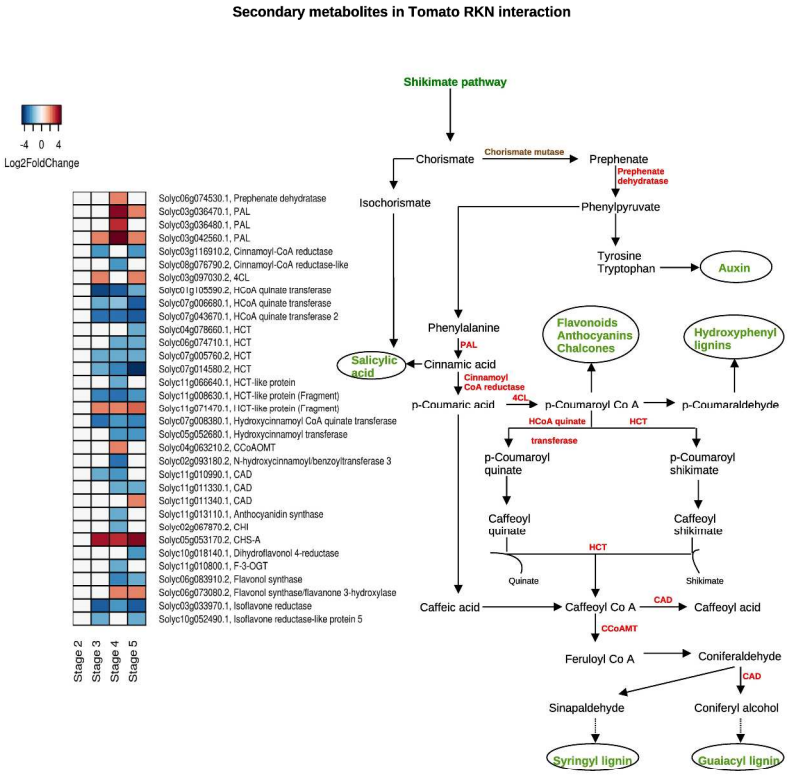

Fig. 4. Schematic representation of gene expression patterns (left) of tomato-DEGs involved in phenylpropanoid biosynthetic pathway (right). Pathway showing DEGs (in red) and end products of pathways (in green) during susceptible response. In heatmap, each row represent a gene and each column represents stage of disease development. Labels on right side of heatmap states gene id followed by annotation. Color key is given on top-left corner of figure. 4CL, 4-hydroxycinnamoylCoA ligase; CAD, cinnamyl alcohol dehydrogenase; CCoAMT, caffeoylCoA-O-methyltransferase; HCT, Hydroxycinnamoyl shikimate/quinate hydroxycinnamoyl transferase; HCoA, Hydroxycinnamoyl Co A; PAL, phenylalanine ammonia lyase.

297x420mm (300 x 300 DPI)

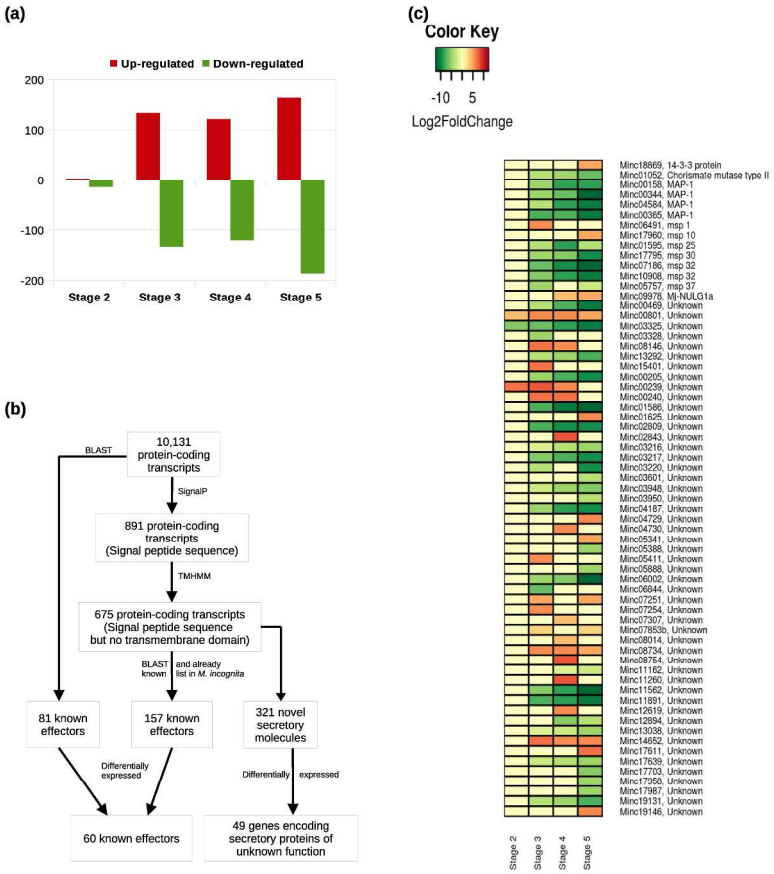

Fig. 5(a) Distribution of significant RKN differentially expressed genes (DEGs) detected at different stages of infection as compared to stage 1 during susceptible response. (b) Workflow summary of bioinformatic strategy used to identify RKN candidate effector genes. (c) Schematic representation of gene expression patterns of RKN-DEGs reported to be involved in parasitism during susceptible response. Each row represents a gene and each column represents stage of disease development. Labels on right side states gene id followed by annotation. Color key is given on top-left corner of figure.

297x420mm (300 x 300 DPI)

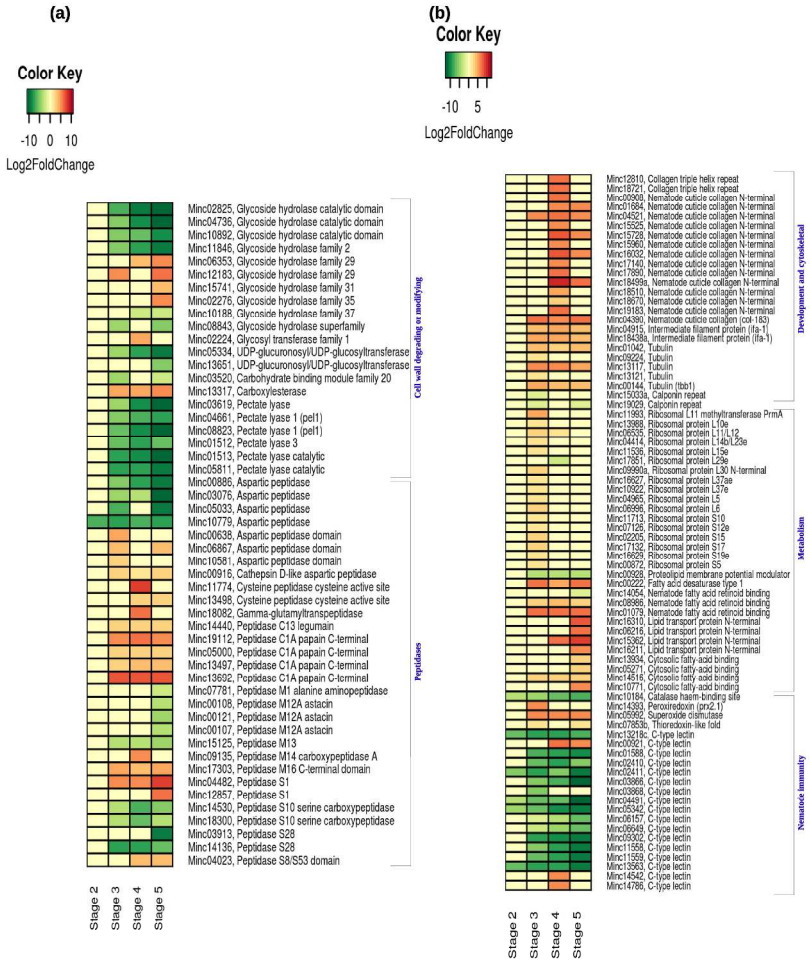

Fig. 6. Schematic representation of gene expression patterns of RKN-DEGs involved in (a) cell wall degradation and peptidase-encoding (b) development, metabolism and nematode immunity, detected during susceptible response. Each row represents a gene and each column represents stage of disease development. Labels on right side of heatmap states gene id followed by annotation. Color key is given on top-left corner of figure.

297x420mm (300 x 300 DPI)

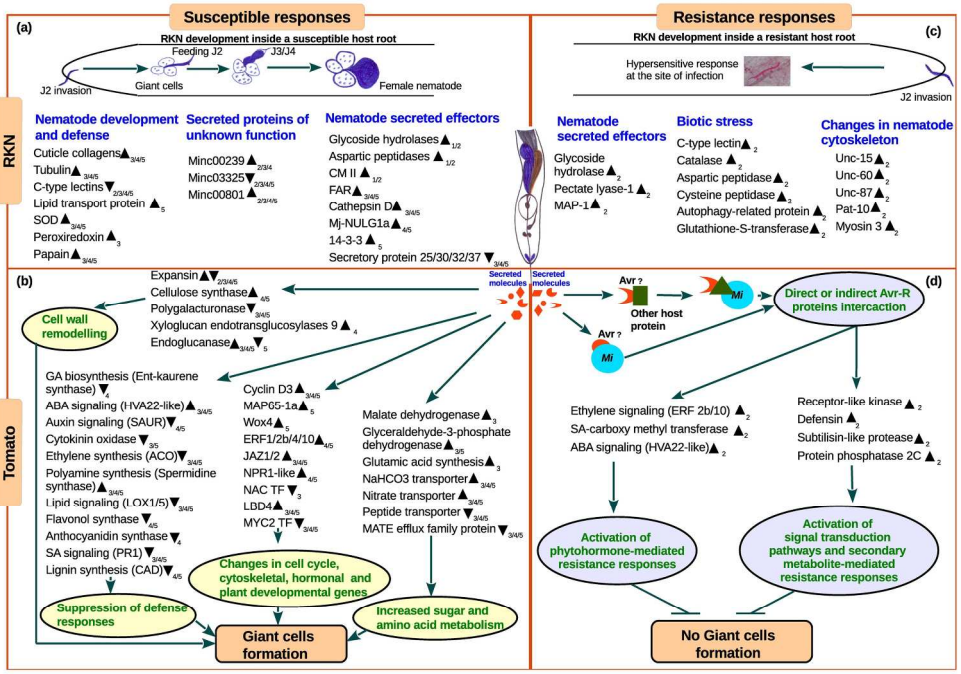

Fig. 7. A model that depicts complex changes in the biochemical processes in both tomato and RKN during susceptible and resistant interactions based on the summary of transcriptome data. (a) Changes in expression of RKN genes during susceptible responses. (b) Changes in expression of tomato genes during susceptible responses. (c) Changes in expression of RKN genes during resistance responses. (d) Changes in expression of tomato genes during resistance responses. The up-arrow head indicates up-regulated genes; down-arrow head indicates down-regulated genes and numerical sub-script in the arrowhead indicates specific stages where the expression was observed. Host metabolic process that are modulated upon RKN-infection are highlighted in colored circles. ABA, abscisic acid; ACO, 1-aminocyclopropane-1-carboxylic acid oxidase; Avr, avirulence protein; CAD, cinnamyl alcohol dehydrogenase; CM II, chorismate mutase type-II; ERF, ethylene responsive transcription factor; FAR, nematode fatty-acid retinol binding protein; GA, gibbrellins; LBD, lateral organ body domain containing transcription factor; LOX, lipoxygenase; MAP-1, Meloidogyne avirulence protein; NAC TF, no apical meristem containing transcription factor; MAP65-1a, microtubule associated protein 65-1a; pat, paralysed arrest two-fold; PR1, pathogenesis-related protein 1; SA, salicylic acid; SOD, superoxide dismutase; unc, uncoordinated; Wox4, WUS homeobox containing gene.

209x148mm (300 x 300 DPI)

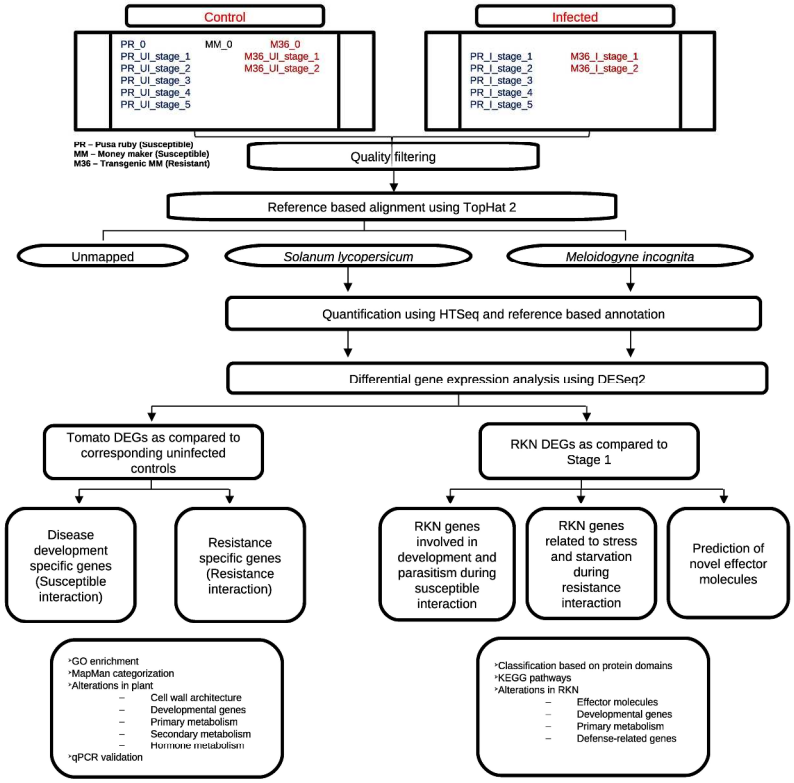

Fig. 8. Workflow summary used for transcriptome data analysis.

297x420mm (300 x 300 DPI)

Table 1. Statistics of good quality reads mapped onto tomato and nematode reference genomes.

Sample	Replicate 1				Replicate 2			
	No. of read pairs aligned onto *Solanum lycopersicum* genome	Percentage read pairs aligned (%)	No. of read pairs aligned onto *Meloidogyne incognita* genome	Percentage read pairs aligned (%)	No. of reads aligned onto *Solanum lycopersicum* genome	Percentage reads aligned (%)	No. of reads aligned onto *Meloidogyne incognita* genome	Percentage reads aligned (%)
PR_stage_0	67,446,974	92.4	10,687	0.0	11,923,705	95.0	498	0.0
PR_UI_stage_1	66,575,269	89.4	21,248	0.0	23,296,422	93.9	1,777	0.0
PR_UI_stage_2	48,847,742	91.6	107	0.0	36,674,766	95.4	1,044	0.0
PR_UI_stage_3	49,304,943	82.7	1,169	0.0	8,761,649	94.0	822	0.0
PR_UI_stage_4	58,326,864	78.4	1,065	0.0	41,281,223	93.8	3,273	0.0
PR_UI_stage_5	78,560,558	90.2	1,111	0.0	39,893,121	92.7	1,672	0.0
PR_I_stage_1	72,787,284	90.7	62,935	0.1	22,781,784	91.2	10,552	0.0
PR_I_stage_2	54,697,086	84.8	102,658	0.2	11,485,953	94.6	8,366	0.1
PR_I_stage_3	76,668,601	90.9	663,329	0.8	29,797,293	91.0	252,817	0.8
PR_I_stage_4	52,626,967	85.8	827,860	1.4	15,107,463	90.1	358,995	2.1
PR_I_stage_5	63,581,675	74.9	5,377,656	6.3	11,078,964	81.2	1,026,425	7.5
MM_stage_0	57,113,244	92.1	114	0.0	50,439,346	93.2	2,658	0.0
M36_stage_0	79,366,778	92.0	205	0.0	23,983,409	95.1	498	0.0
M36_UI_stage_1	24,077,820	88.4	19,314	0.1	36,635,563	94.0	2,657	0.0
M36_UI_stage_2	20,417,489	74.6	39,740	0.1	34,522,313	95.4	779	0.0
M36_I_stage_1	82,496,591	89.9	54,895	0.1	15,613,149	94.5	12,528	0.1
M36_I_stage_2	78,517,115	90.5	89,928	0.1	32,888,657	94.7	47,024	0.1

- *Replicate 1 – paired end reads, Replicate 2 – single end reads; UI – Uninfected, I – Infected*
- *PR – Pusa Ruby (susceptible cultivar), MM – Money Maker (susceptible cultivar), M36 – Transgenic MM (resistant line)*